Molecular Biology of the Cell
Vol. 17, 3318–3328, July 2006

Annexin A4 Self-Association Modulates General Membrane Protein Mobility in Living Cells[V]

Alen Piljić and Carsten Schultz

Gene Expression Programme, European Molecular Biology Laboratory, 69117 Heidelberg, Germany

Submitted January 17, 2006; Revised April 27, 2006; Accepted April 28, 2006
Monitoring Editor: Jean Gruenberg

Annexins are Ca^{2+}-regulated phospholipid-binding proteins whose function is only partially understood. Annexin A4 is a member of this family that is believed to be involved in exocytosis and regulation of epithelial Cl^- secretion. In this work, fluorescent protein fusions of annexin A4 were used to investigate Ca^{2+}-induced annexin A4 translocation and self-association on membrane surfaces in living cells. We designed a novel, genetically encoded, FRET sensor (CYNEX4) that allowed for easy quantification of translocation and self-association. Mobility of annexin A4 on membrane surfaces was investigated by FRAP. The experiments revealed the immobile nature of annexin A4 aggregates on membrane surfaces, which in turn strongly reduced the mobility of transmembrane and plasma membrane associated proteins. Our work provides mechanistic insight into how annexin A4 may regulate plasma membrane protein function.

INTRODUCTION

The annexin family consists of ubiquitous proteins that interact with phospholipids in a Ca^{2+}-dependent manner. Annexins are structurally distinct compared with other Ca^{2+}-binding proteins. Each annexin consists of an N-terminal domain and a typical core domain. The latter binds Ca^{2+} and phospholipids and is comprised of four annexin repeats (eight in case of annexin A6), each ~70 residues in size. The annexin core is conserved among all members of the annexin family. In contrast, N-terminal domains are variable in length and are believed to regulate annexin functions (Gerke and Moss, 2002). By mediating intracellular Ca^{2+} signals, annexins have been shown to play a role in a variety of cellular processes. Some annexins have been reported to act as membrane scaffolds or to be involved in membrane trafficking and organization (Rescher and Gerke, 2004; Gerke *et al.*, 2005). By blocking the access to lipid substrates, they may regulate enzyme activity like that of phospholipase A_2 (Davidson *et al.*, 1987). Other annexins modulate ion channel activity (Gerke and Moss, 2002) or are believed to conduct Ca^{2+} ions across membranes by themselves (Kourie and Wood, 2000). In addition, some members of the annexin family have extracellular and nuclear functions (Rescher and Gerke, 2004; Gerke *et al.*, 2005).

This article was published online ahead of print in *MBC in Press* (http://www.molbiolcell.org/cgi/doi/10.1091/mbc.E06–01–0041) on May 10, 2006.

[V] The online version of this article contains supplemental material at *MBC Online* (http://www.molbiolcell.org).

Address correspondence to: Carsten Schultz (schultz@embl.de).

Abbreviations used: $[Ca^{2+}]_i$, intracellular calcium concentration; CaMKII, multifunctional calcium/calmodulin-dependent protein kinase II; CaCC, calcium-activated chloride conductance; CF, cystic fibrosis; CYNEX4, cyan-yellow-labelled annexin A4; ECFP, enhanced cyan fluorescent protein; EYFP, enhanced yellow fluorescent protein; FRET, fluorescence resonance energy transfer; PLCδ1, phospholipase Cδ1.

Mammalian annexin A4 was first identified as Ca^{2+} and lipid-binding porcine protein II (Gerke and Weber, 1984; Weber *et al.*, 1987). Later it was shown to self-associate on membrane surfaces and to aggregate phospholipid membranes (Zaks and Creutz, 1991). Moreover, annexin A4 formed trigonal crystals that assembled in ordered two-dimensional (2D) arrays on membrane surfaces (Newman *et al.*, 1991; Zanotti *et al.*, 1998; Kaetzel *et al.*, 2001). Kaetzel *et al.* (2001) also showed that annexin A4 promoted vesicle aggregation in vitro. This activity was inhibited when the protein was phosphorylated by protein kinase C (PKC). Additionally, annexin A4 was shown to be part of a protein complex believed to have a role in synaptic exocytosis (Willshaw *et al.*, 2004). These studies implied a role for annexin A4 in the regulation of vesicle trafficking.

It has been demonstrated that annexin A4 modulates Ca^{2+}-activated Cl^- conductance (CaCC) in colonic T84 epithelial cells (Chan *et al.*, 1994; Kaetzel *et al.*, 1994; Xie *et al.*, 1996). CaCC localizes to the apical membrane of epithelial cells. It is activated by Ca^{2+} and/or phosphorylation by multifunctional Ca^{2+}/calmodulin-dependent protein kinase II (CaMKII) and is inhibited not only by annexin A4, but also by $Ins(3,4,5,6)P_4$ and cellular phosphatases (Vajanaphanich *et al.*, 1994; Xie *et al.*, 1996, 1998; Carew *et al.*, 2000; Ho *et al.*, 2001). Accordingly, the CaCC in lung epithelia is a potential pharmacological target in cystic fibrosis (CF), because other Cl^- channels like the cystic fibrosis transmembrane conductance regulator (CFTR) and the outwardly rectifying Cl^- channel (ORCC) are either not abundant or inactive in epithelia of CF patients, respectively. Thus, it is essential to understand the mechanism underlying regulation of CaCC, including the role of annexin A4, in order to develop future medication for CF.

Members of the annexin family are expressed in various cell types and tissues. Annexin A4 is predominantly found in epithelial cells (Dreier *et al.*, 1998), mostly below the apical membrane (Kaetzel *et al.*, 1989, 1994; Mayran *et al.*, 1996). Few studies of annexin A4 localization have been conducted in cultured cells. Immunofluorescence experiments with human fibroblasts revealed that annexin A4 translocated to the inner surface of the nuclear membrane and the plasma

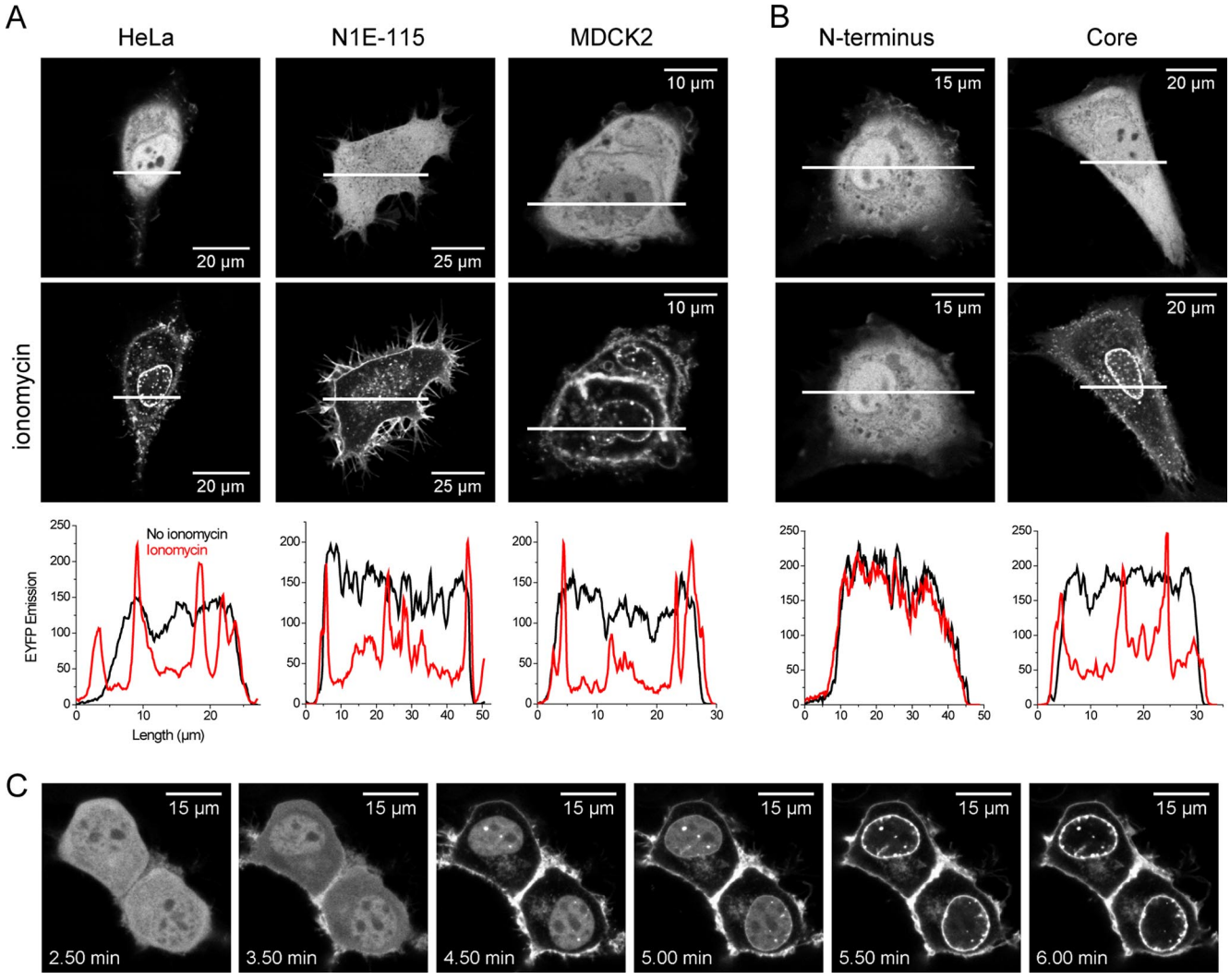

Figure 1. Annexin A4 localization and translocation in living cells. (A) EYFP-annexin A4 expressed in HeLa, N1E-115, and MDCK2 cells translocated to cell membranes upon Ca^{2+} elevation with ionomycin. The onset and duration of translocation was variable between experiments. In some cases protein translocation started immediately and in others with a delay of up to 5 min. (B) The core of annexin A4 behaved like wild-type protein in HeLa cells. Graphs show protein distribution across cells. White bars indicate position of the measurement. (C) Sequence of images showing annexin A4 translocation in the cytosol and delayed translocation in the nucleus of N1E-115 cells (from Supplementary Video 1). Images were taken every 10 s. Ionomycin was added after 2.5 min.

membrane upon treatment of cells with Ca^{2+} ionophore A23187 (Barwise and Walker, 1996; Raynal *et al.*, 1996). The goal of our study was to analyze the dynamic behavior of annexin A4 in living cells. Using fluorescent protein labeling and imaging techniques, we studied annexin A4 translocation to cell membranes and its self-association on membrane surfaces. Additionally, we investigated the mobility of membrane-bound annexin A4 and its effect on the mobility of various membrane proteins.

MATERIALS AND METHODS

Construction of Plasmids

The cDNA for human annexin A4 (Image: 268747) was obtained from LGC Promochem (Wesel, Germany). To construct the ECFP-annexin A4 and EYFP-annexin A4 fusions, the coding sequence of annexin A4 was amplified by PCR. The resulting product was digested with EcoRI and BamHI and inserted into the pEYFP-C1 and pECFP-C1 vectors (Clontech, Palo Alto, CA; ECFP had two additional mutations, as described in Llopis *et al.*, 2000). To generate the annexin A4-ECFP and annexin A4-EYFP fusions, annexin A4 was amplified by PCR. The product was digested with EcoRI and BamHI and ligated into pEYFP-N1 and pECFP-N1 vectors (Clontech). EYFP tagged with the annexin A4 16 N-terminal amino acids was generated using primers that encode the 16 amino acids flanked with EcoRI and BamHI restriction sites. The primers were 5′ phosphorylated with T4 polynucleotide kinase, annealed, digested with restriction enzymes, and inserted into the pEYFP-N1 vector (Clontech). To construct the EYFP-annexin A4 core fusion, the sequence encoding the core of annexin A4 was amplified by PCR. The resulting product was digested with EcoRI and BamHI and inserted into the pEYFP-C1 vector (Clontech). To construct the EYFP-annexin A4-ECFP double fusion (CYNEX4), EYFP was amplified by PCR. The product was digested with BglII and EcoRI and ligated into the pECFP-N1-annexin A4 vector (construction described above).

YFP-$PH_{PLC\delta1}$ was provided by Kees Jalink (The Netherlands Cancer Institute, Amsterdam), ErbB1-EYFP by Philippe Bastiaens (European Molecular Biology Laboratory, Heidelberg), CHRM2-EYFP and GPI-EYFP by Rainer Pepperkok (European Molecular Biology Laboratory, Heidelberg). pEYFP-Mem was obtained from Clontech.

Cell Culture and Transfection

HeLa and N1E-115 cells were passaged and maintained in DMEM supplemented with 10% fetal bovine serum (FBS) and 0.1 mg/ml primocin. MDCK2 cells were maintained in MEM supplemented with 5% FBS, 2 mM L-glutamine, and 0.1 mg/ml primocin. For imaging experiments, cells were plated

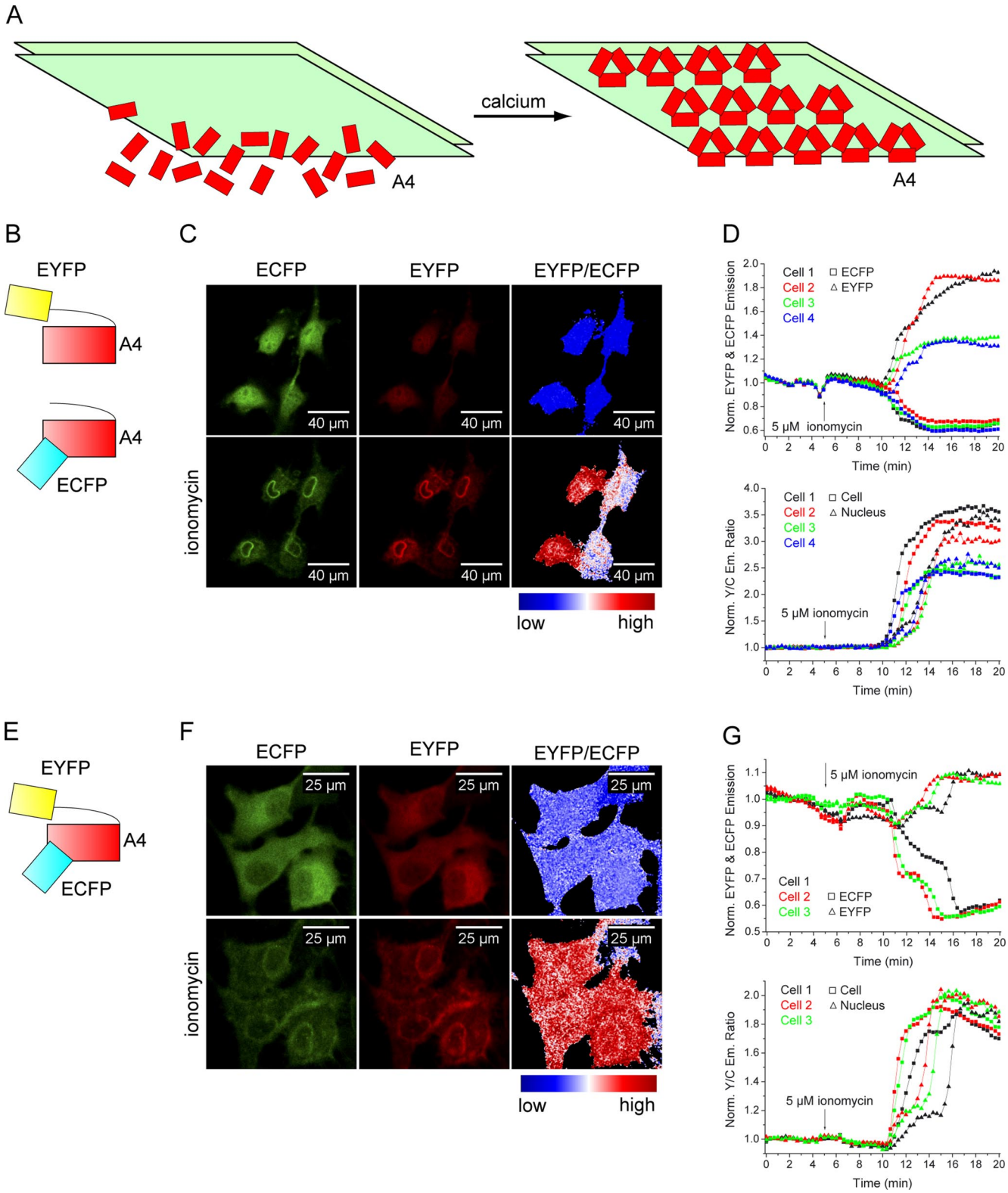

Figure 2. Annexin A4 self-association on the membrane surface. (A) Schematic representation of Ca^{2+}-induced annexin A4 trimer association into 2D crystal arrays on the membrane surface. (B) Annexin A4 was labeled C- or N-terminally with ECFP or EYFP. Fusions were used in different combinations in order to determine if annexin A4 self-associates on the surface of cell membranes. (C) Images of annexin A4-ECFP and annexin A4-EYFP cotransfected HeLa cells with the corresponding false color ratio image, before and after ionomycin addition. (D) EYFP fluorescence increased, whereas ECFP decreased as fusion proteins translocated to the membranes of the four cells shown in C. The resulting EYFP/ECFP ratio increase was measured in the whole cell or only in the nucleus. Similarly high FRET signal upon translocation was obtained regardless if the fusions were both C-terminal (as shown), N-terminal, or mixed (unpublished data). (E) CYNEX4, annexin A4 N-terminally labeled with EYFP and C-terminally with ECFP. (F) ECFP and EYFP emission of CYNEX4 expressed in HeLa cells and

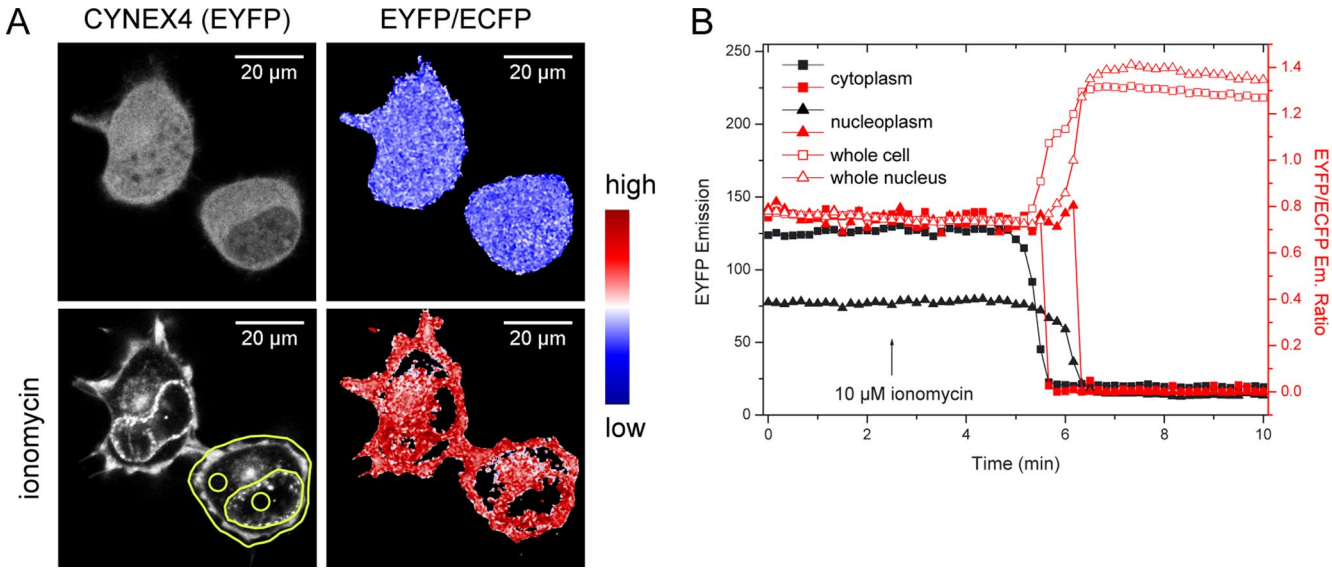

Figure 3. Annexin A4 self-association in N1E-115 cells. (A) EYFP emission of CYNEX4 and EYFP/ECFP emission ratio before and after ionomycin-induced translocation (Supplementary Video 3). (B) EYFP emission and EYFP/ECFP ratio measured over time in regions indicated in A. While the protein is translocating and EYFP fluorescence signal dropping in the cytoplasm or nucleoplasm, the FRET ratio is not increasing as in the whole cell or whole nucleus. This indicates that annexin A4 self-association takes place only on cell membranes.

in 35-mm MatTek chambers (Ashland, MA) and transfected at 50–70% confluency. HeLa and N1E-115 cells were transfected with FuGENE 6 reagent (Roche, Mannheim, Germany). MDCK2 cells were transfected with either FuGENE 6 or Lipofectamine 2000 (Invitrogen, Carlsbad, CA). Transfections were performed in Opti-MEM (Invitrogen) according to the manufacturer's instructions. Cells were washed 12–24 h after transfection and incubated in imaging medium (20 mM HEPES, pH 7.4, 115 mM NaCl, 1.2 mM $CaCl_2$, 1.2 mM $MgCl_2$, 1.2 mM K_2HPO_4, 2 g/l D-glucose) at 37°C with 5% CO_2 for 1–2 h before imaging.

Western Blotting

Cells were washed in phosphate-buffered saline and lysed in lysis buffer (50 mM HEPES, pH 7.5, 150 mM NaCl, 1 mM EDTA, 1 mM EGTA, 10% glycerol, 1% Triton X-100) supplemented with protease and phosphatase inhibitor cocktails (Sigma, Steinheim, Germany). The lysates were centrifuged to remove cell debris, and supernatants were stored at −70°C. Samples were separated by SDS-PAGE, and afterward proteins were transferred onto an Immobilon PVDF membrane (Millipore, Bedford, MA). An anti-annexin A4 mouse monoclonal antibody (BD Biosciences, San Diego, CA) and HRP-conjugated goat anti-mouse IgG (Bio-Rad, Richmond, CA) were used to detect annexin A4.

Confocal Microscopy and Image Analysis

Images were acquired on a Leica TCS SP2 AOBS microscope (Leica Microsystems, Heidelberg, Germany) with an HCX PL APO lbd.BL 63.0 × 1.40 oil objective at 30°C. Annexin A4 localization and translocation images were obtained with the following microscope settings: ECFP was excited with the 458-nm laser line, and emission was sampled between 470 and 500 nm; EYFP was excited with the 515-nm laser line, and emission was sampled between 525 and 600 nm (pinhole 2.62 airy). Images were background-corrected and smoothed with a median filter using ImageJ software (http://rsb.info.nih.gov/ij/).

ECFP and EYFP excitation and emission settings for acceptor bleaching experiments were the same as above (pinhole fully opened, 5.23 airy). EYFP was bleached in a rectangular region with the 515-nm laser line at 2/3 laser power after 10 iterations. ECFP image was acquired before and after bleaching of EYFP. Images were background corrected and smoothed with a median filter, and a threshold was applied. Fluorescence resonance energy transfer (FRET) efficiency was calculated as described before (Wouters *et al.*, 2001). All operations were done using ImageJ.

To calculate EYFP/ECFP ratio, ECFP was excited with a 20-mW 405-nm diode laser. ECFP was sampled between 470 and 510 nm and EYFP between 520 and 540 nm. Background-subtracted EYFP and ECFP images were smoothed with a median filter and thresholded. EYFP images were then divided by ECFP images using ImageJ. For calcium-imaging experiments 7–15 μM Fura red/AM (Molecular Probes, Eugene, OR) was loaded into cells for 30–40 min. Cells were then washed and incubated in fresh imaging medium for 15 min before acquisition. Fura red was also excited with a 405-nm laser line, and emission was sampled from 620 to 750 nm. Both ECFP and EYFP images were corrected for the Fura red bleed through before EYFP/ECFP ratio could be calculated. Experiments with high number of cells (>50) were acquired using an HCX PL APO 40.0 × 1.25 oil objective. The microscope settings and image processing were identical to those described above.

Fluorescence recovery after photobleaching (FRAP) experiments were done on a Leica TCS SP2 AOBS microscope (Leica Microsystems) using an HCX PL APO lbd.BL 63.0 × 1.40 oil objective at room temperature (22°C). The CHRM2-EYFP and ErbB1-EYFP constructs needed more time to express and localize in the plasma membrane. Photobleaching experiments with these constructs were therefore done 48–60 h after transfection. EYFP was bleached in a rectangular region (3 × 3 μm) with the 476-, 488-, 496-, and 515-nm laser lines at 280-mW Kr/Ar laser power in a single scan. Recovery of EYFP fluorescence between 525 and 600 nm was then monitored at low laser power with the 515-nm laser line. The images were background corrected and smoothed with a median filter. Recovery in the bleached region was measured and corrected for bleaching that occurred during acquisition at low laser power. The recovery (mobile fraction) was then calculated as described before (Lippincott-Schwartz *et al.*, 2001).

Supplementary Material

Supplementary Video 1 shows EYFP-annexin A4 translocation in N1E-115 cells. Supplementary Videos 2 and 3 show CYNEX4 translocation/self-association in HeLa and N1E-115 cells, respectively. Translocation was in all cases induced with 5–10 μM ionomycin. Fluorescence emission is shown in gray. Emission ratios are shown in false color, with blue representing low and red representing high emission ratio.

RESULTS

Annexin A4 Translocation in Living Cells

Annexin A4 was expressed as an N- or C-terminal fusion protein with ECFP or EYFP. The constructs were expressed in three different cell lines: HeLa, MDCK2, and N1E-115 neuroblastoma cells. All fusions were evenly distributed in the cytoplasm and the nucleus. The cells were then treated with the Ca^{2+} ionophore ionomycin. One to 5 min after addition, annexin A4 fusion proteins translocated to the

Figure 2 (cont). EYFP/ECFP ratio image before and after ionomycin treatment (Supplementary Video 2). (G) ECFP and EYFP traces and EYFP/ECFP ratio of CYNEX4 in the cells shown in F.

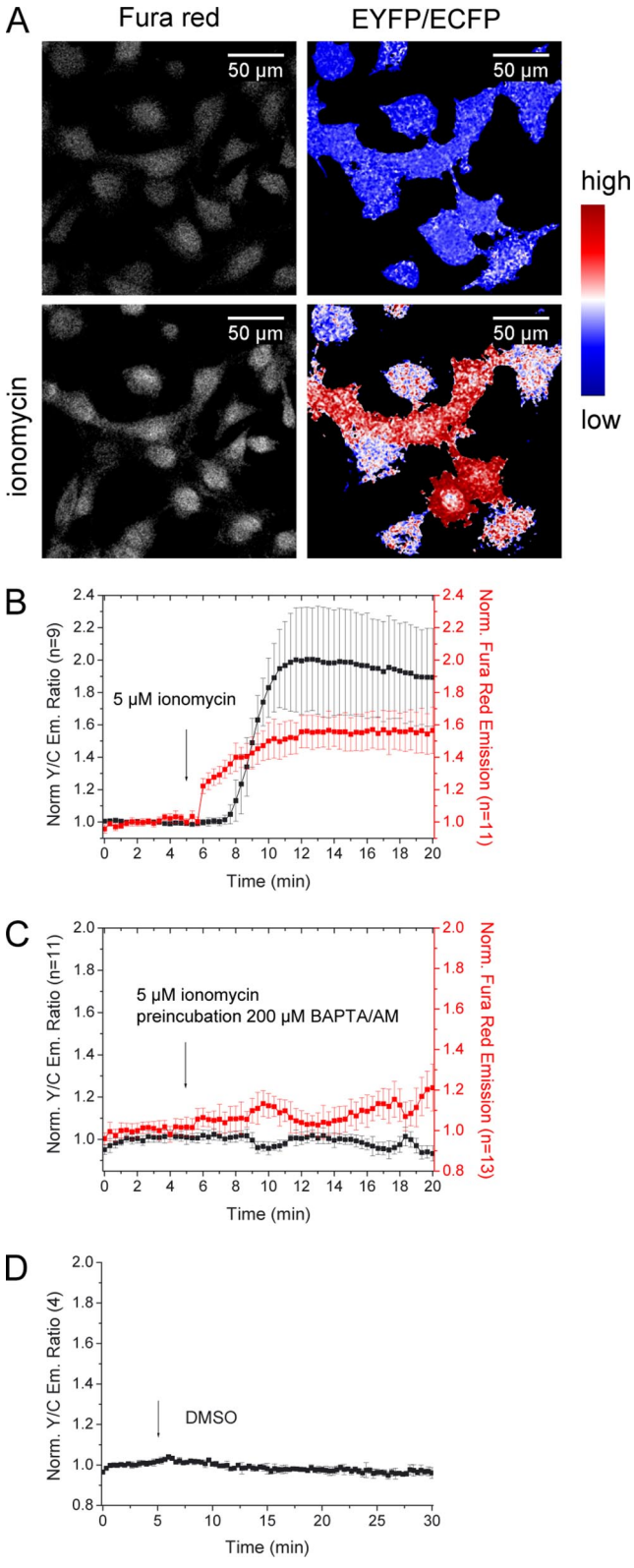

Figure 4. Dual parameter imaging using CYNEX4. (A) HeLa cells expressing CYNEX4 were loaded with Fura red and treated with ionomycin. (B) $[Ca^{2+}]_i$ increased before annexin A4 translocated to the membrane. (C) Cells preincubated with BAPTA/AM showed no Ca^{2+} increase, and annexin A4 translocation was therefore absent. (D) Vehicle failed to induce translocation. Error bars, SD.

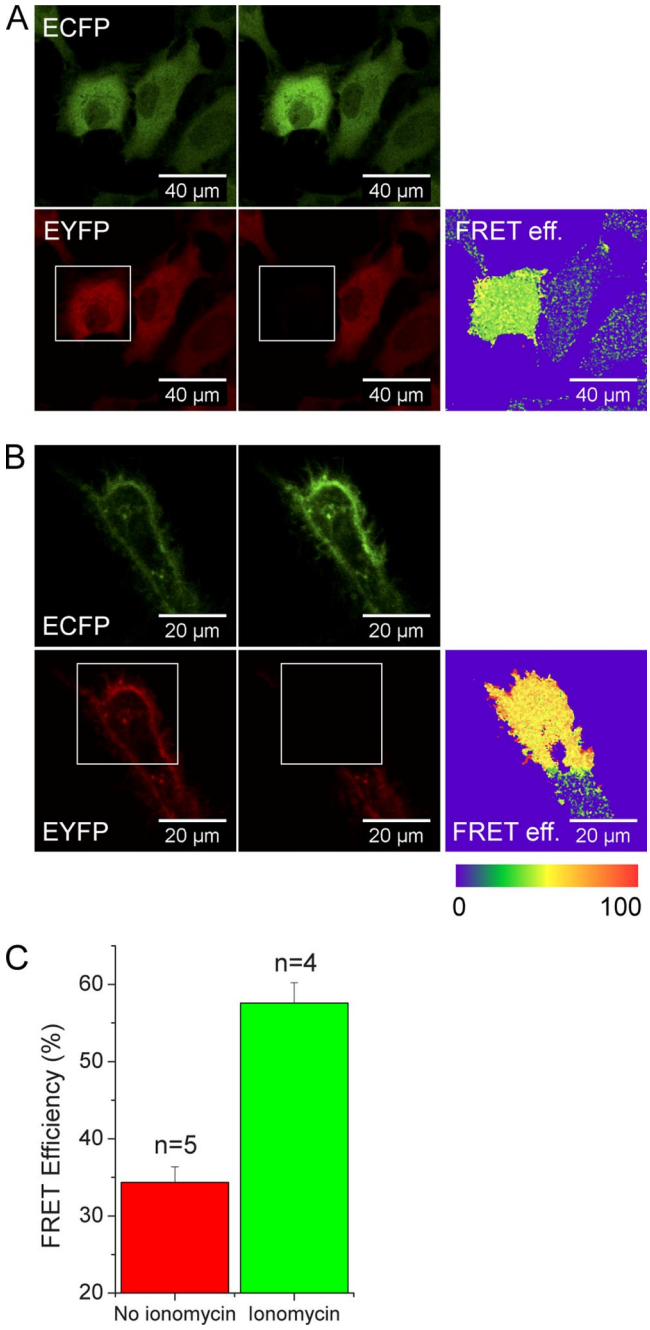

Figure 5. Acceptor bleaching of CYNEX4. (A) Acceptor bleaching of unstimulated HeLa cells. (B) Acceptor bleaching of cells treated with ionomycin and after CYNEX4 translocation to membranes. (C) Calculated FRET efficiencies in untreated and ionomycin-treated cells. Error bars, SD of 4–5 experiments.

plasma membrane and subsequently to the nuclear membrane in all three cell types (Figure 1A). Nuclear membrane staining was often speckled. In addition, the fusions also bound to membrane structures in the perinuclear region and vesicles in the cytoplasm. The cytosolic pool of the protein always translocated before the nuclear pool (Figure 1C and Supplementary Video 1). Both C- and N-terminal annexin A4-fluorescent protein fusions behaved in the same way. Translocation in HeLa and MDCK2 cells was also induced by 8-Br-A23187. Agents that elevated intracellular calcium

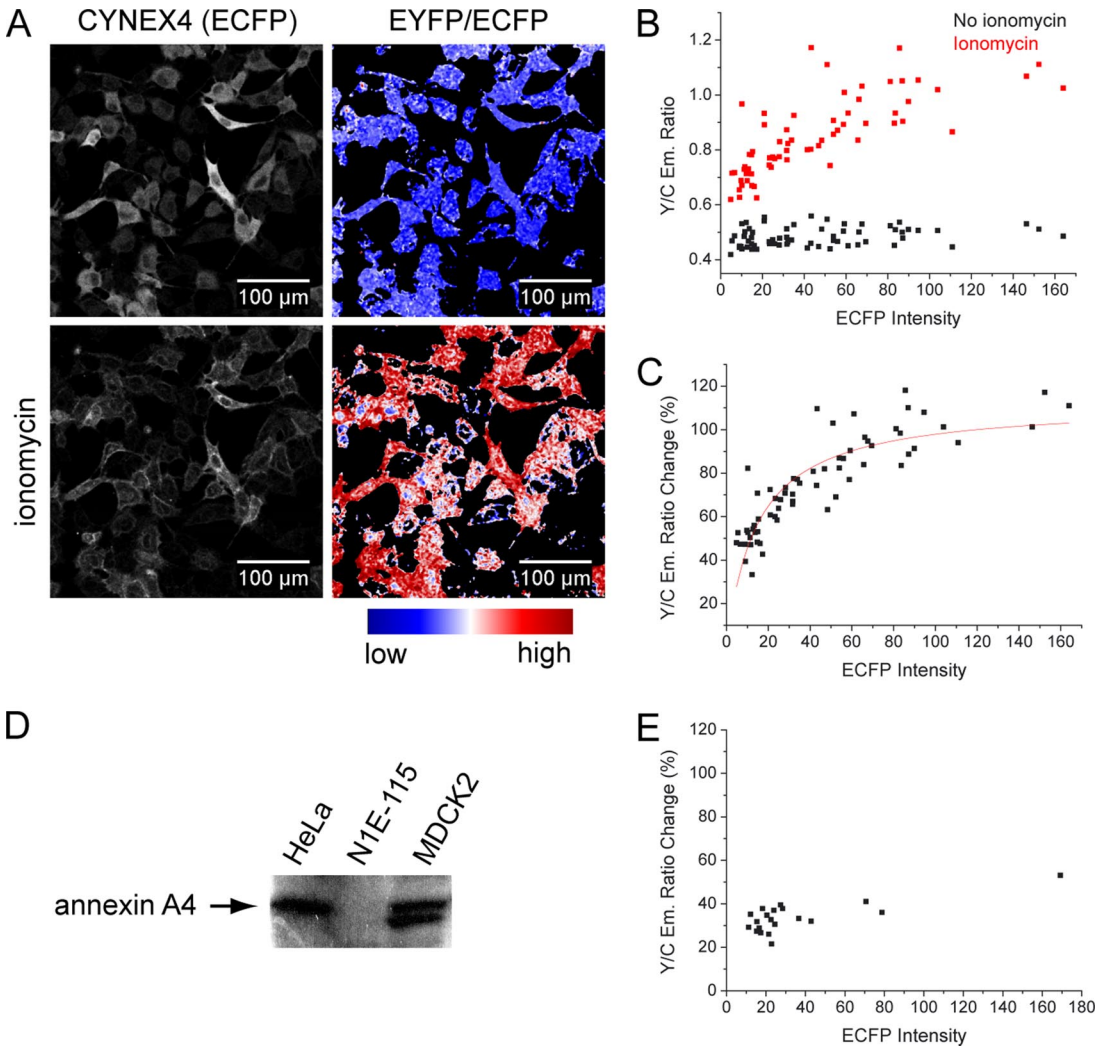

Figure 6. FRET dependency on CYNEX4 expression levels. (A) EYFP emission of CYNEX4 expressed in HeLa cells and EYFP/ECFP emission ratio before and after ionomycin-induced translocation. (B) EYFP/ECFP emission ratio is plotted against the fluorescence in the ECFP channel (indicative of protein expression level) for each HeLa cell. (C) EYFP/ECFP emission ratio change [$(Y/C_{ionomycin} - Y/C_{no\ ionomycin})/Y/C_{no\ ionomycin} * 100$] correlated to ECFP intensity in HeLa cells. Because the FRET increase is a consequence of protein–protein interaction, the data were fitted with a simple hyperbolic binding function. (D) A Western blot confirming annexin A4 expression in HeLa and MDCK2 cells. The second band in MDCK2 lane may be annexin A4, whose N-terminal domain has been cleaved by proteases. (E) EYFP/ECFP emission ratio change correlated to ECFP intensity in N1E-115 cells.

concentration ($[Ca^{2+}]_i$) transiently, such as histamine or ATP, were not effective when tested in HeLa cells (unpublished data).

To understand the contribution of the annexin A4 domains to Ca^{2+}-induced translocation, two additional constructs were prepared. The first consisted of the 16 N-terminal amino acids of annexin A4 (N-terminal regulatory sequence) fused to EYFP. The second was a fusion of EYFP and the annexin A4 core that lacked the N-terminal regulatory sequence. The core translocated to cell membranes upon ionomycin treatment, just as the full-length protein. The N-terminal amino sequence fused to EYFP remained cytosolic (Figure 1B). The experiment demonstrated that in vivo the core of the protein, but not the N-terminal domain, is required for annexin A4-membrane interaction.

Annexin A4 Self-Association on Membrane Surfaces

Annexin A4 is known to form 2D trimer-based arrays on membrane surfaces in the presence of Ca^{2+} (Newman *et al.*, 1991; Kaetzel *et al.*, 2001; Figure 2A). Because this phenomenon has previously been observed only in vitro, we wanted to test if such protein self-association occurs in vivo. First, we used an intermolecular FRET approach, similar to that previously described for lipid-sensing pleckstrin homology (PH) domains by van der Wal *et al.* (2001). ECFP- and EYFP-labeled annexin A4 constructs were cotransfected and expressed in HeLa cells. Ionomycin was used to elevate $[Ca^{2+}]_i$. On protein translocation to membranes, the EYFP/ECFP emission ratio increased up to 300% (Figure 2, B–D), suggesting that the molecules packed so tightly that very strong FRET could occur. However, unspecific and random interaction could not be excluded using this approach.

To avoid the necessary selection of cells that coexpressed both constructs at similar levels, we prepared an additional translocation probe, intramolecularly tagged with both EYFP and ECFP at the N- and C-terminus, respectively (cyan/yellow labeled annexin A4 [CYNEX4]; Figure 2E). In the past, a similar sensor was described that measured phos-

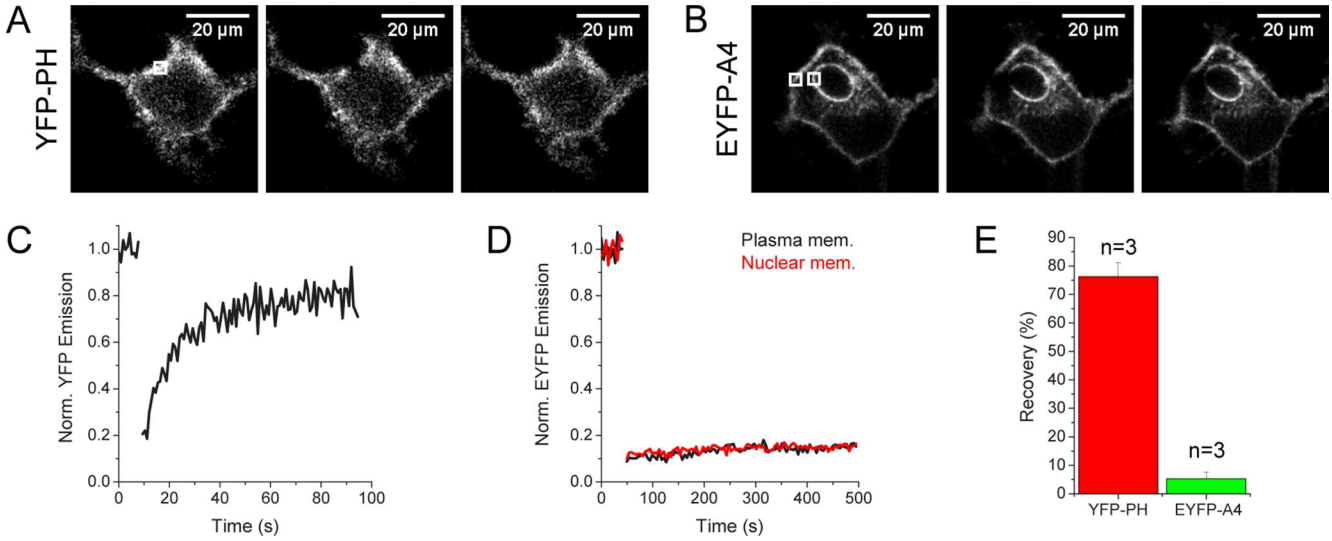

Figure 7. Comparison of YFP-$PH_{PLC\delta1}$ and EYFP-annexin A4 mobility by FRAP. (A) Photobleaching of YFP-$PH_{PLC\delta1}$ expressed in HeLa cells. (B) Photobleaching of EYFP-annexin A4 expressed and translocated in HeLa cells. A region in the plasma membrane and in the nuclear membrane was bleached. (C and D) EYFP fluorescence recovery in the bleached regions of the experiments shown in A and B, respectively. (E) Average recovery after photobleaching of the $PH_{PLC\delta1}$ domain and membrane bound annexin A4. Error bars, SD of three experiments.

phatidylinositol 4,5-bisphosphate ($PI(4,5)P_2$) breakdown (Violin *et al.*, 2003). As expected, CYNEX4 eliminated the problems of coexpression, while still showing the same localization and translocation properties. However, CYNEX4 was less abundant in the nucleus in comparison to single fluorescent protein fusions. Ratiometric measurements with the novel sensor were performed in all three cell lines. Figure 2, F and G (and Supplementary Video 2), depicts the results in HeLa cells. Results in MDCK2 and N1E-115 cells were similar (unpublished data). CYNEX4 reported up to 150% increase of EYFP/ECFP ratio upon translocation.

Experiments with HeLa cells seemed to show that FRET increased also in the cytosol, not only on cell membranes. However, what appeared to be cytosolic fluorescence was in fact membrane signals below and above the imaging plane in flat HeLa cells. Experiments in high, pyramid shaped N1E-115 cells, where such membrane signal contribution did not occur with our microscopy settings (see *Materials and Methods*), showed that FRET did not increase in the cytosol before probe translocation (Figure 3, A and B; Supplementary Video 3). This indicated that annexin A4 self-association indeed took place only on cell membrane surfaces.

Because annexin A4 translocation is Ca^{2+}-dependent, we next tried to monitor protein translocation in parallel to Ca^{2+} levels in HeLa cells. CYNEX4 was used to detect annexin A4 translocation, whereas Fura red reported changes in $[Ca^{2+}]_i$. As expected, the experiment showed that $[Ca^{2+}]_i$ increased before annexin A4 translocation (Figure 4, A and B). Cells preincubated with BAPTA/AM exhibited no Ca^{2+} elevation and protein translocation was therefore absent (Figure 4C). In addition, cells were imaged for 30 min to demonstrate that translocation is not the result of vehicle addition or phototoxicity (Figure 4D).

To determine FRET efficiencies (E), we examined CYNEX4 by acceptor bleaching. The sensor exhibited a significant level of FRET ($E = 34.4 \pm 2.0\%$; ±SD, $n = 5$) in the cytosol without Ca^{2+} stimulation that further increased after Ca^{2+}-induced translocation to membranes ($E = 57.6 \pm 2.6\%$; ±SD, $n = 4$; Figure 5, A–C).

To distinguish specific annexin A4 association from random, diffusion-limited interaction, we then compared the FRET increase in cells expressing different amounts of CYNEX4. As before, CYNEX4 was expressed in HeLa cells, and translocation was induced with ionomycin. We used fluorescence intensity in the ECFP channel before ionomycin stimulation as a measure of CYNEX4 expression levels. The ECFP intensity was then correlated to EYFP/ECFP ratio changes in over 60 cells (Figure 6, A–C). As expected, the FRET ratio before translocation was independent of the protein expression level, indicating that the energy is transferred intramolecularly. On translocation, the FRET ratio increased. The minimal ratio change in cells expressing CYNEX4 very weakly was 30%. However, the EYFP/ECFP emission ratio was not independent of the CYNEX4 concentration and rose up to 120% in cells expressing high levels of CYNEX4. This FRET distribution could not be observed in N1E-115 cells (Figure 6E) and can be explained with the simple fact that endogenous annexin A4 can interact and compete with CYNEX4. We verified by Western blotting that endogenous annexin A4 is present in HeLa cells but not in N1E-115 cells (Figure 6D). Therefore, at low CYNEX4 expression levels in HeLa cells, the contribution of unlabeled annexin A4 in arrays is more significant and leads to lower FRET increases. At high CYNEX4 levels, labeled annexin A4 becomes more abundant in arrays and the FRET ratio increase is therefore larger. These results in living cells support the annexin A4 self-association hypothesis.

Annexin A4 Mobility on Membrane Surfaces

The above experiments showed that annexin A4 molecules interact when associated with membranes in living cells. However, FRET experiments cannot reveal the nature of annexin–annexin interaction on the membrane surface. Is the protein only forming trimers or do these trimers additionally assemble in 2D crystal arrays? In case of 2D arrays protein mobility should be low compared with nonaggregating and freely diffusing protein complexes. Therefore, we used FRAP to address this question. We compared annexin A4 mobility to another membrane-docking protein, the PH

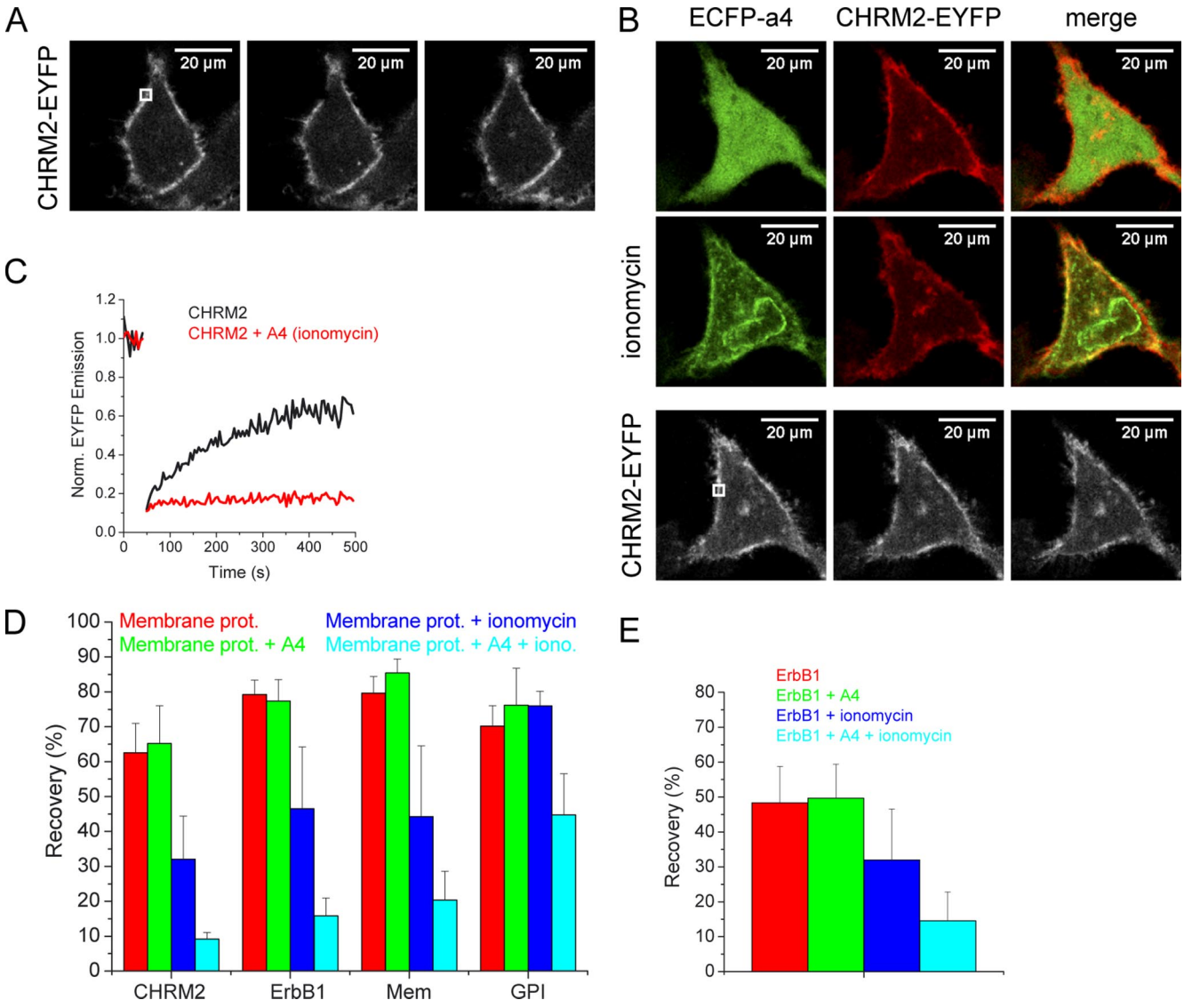

Figure 8. Annexin A4 effect on membrane protein mobility. (A) Photobleaching of CHRM2-EYFP in HeLa cells. (B) Photobleaching of CHRM2-EYFP in HeLa cells coexpressing ECFP-annexin A4 after ionomycin-induced annexin A4 translocation. (C) Representative traces of CHRM2-EYFP fluorescence recovery in the bleached region of the HeLa cells expressing only the receptor, or both the receptor and annexin A4 (translocated to the membrane using ionomycin), as in A and B. (D) Average recovery after photobleaching of four different membrane proteins (CHRM2-EYFP, ErbB1-EYFP, EYFP-Mem, and GPI-EYFP), expressed alone or together with ECFP-annexin A4 in HeLa cells, with or without ionomycin treatment. Error bars, SD of 3–5 experiments. (E) Average recovery after photobleaching of ErbB1-EYFP expressed alone or together with ECFP-annexin A4 in N1E-115 cells, with or without ionomycin treatment. Error bars, SD of 4–9 experiments.

domain of phospholipase Cδ1 (YFP-$PH_{PLC\delta1}$; Figure 7, A–E). The mobile fraction of the PH domain in the plasma membrane was 76.2 ± 5.0% (±SD, n = 3). On the other hand, the recovery of annexin A4 on the membrane reached only 5.3 ± 2.4% (±SD, n = 3), observed over a much larger time span. This clearly demonstrates that the protein is almost completely immobile on the plasma and the nuclear membrane surface. Therefore it is likely that annexin A4 forms highly ordered arrays on membrane surfaces in vivo, as previously described in vitro.

Annexin A4 Inhibits Membrane Protein Mobility upon Ca^{2+} Elevation

A logical consequence of annexin A4 array formation might be the restriction of diffusion of other membrane proteins, especially because annexin A4 was shown to reduce the rate of lateral lipid diffusion in planar bilayers (Gilmanshin *et al.*, 1994). We therefore compared the mobility of membrane proteins before and after ionomycin-induced annexin A4 translocation to the plasma membrane in cells that overexpressed ECFP-annexin A4. Four EYFP-labeled membrane proteins were chosen: a G-protein–coupled receptor (cholinergic receptor, CHRM2-EYFP), a receptor tyrosine kinase (EGF receptor, ErbB1-EYFP), an EYFP protein that localizes to the inner leaflet of the plasma membrane (EYFP-Mem, EYFP fused to the 20 N-terminal amino acids of neuromodulin bearing a palmitoylation sequence), and an EYFP protein that localizes to the outer leaflet of the plasma membrane (glycosylphosphatidylinositol, GPI-EYFP). First, HeLa cells were transfected with these constructs and their mobility after photobleaching was measured with and without iono-

mycin treatment (Figure 8, A and C). The experiments were then repeated with ECFP-annexin A4 coexpressed with the membrane proteins (Figure 8, B and C). The FRAP experiments revealed a strong annexin A4 effect on the mobility of all tested membrane proteins except GPI-EYFP, which localized to the outer leaflet of the plasma membrane and was therefore not expected to be strongly restricted by a grid that forms on the inner leaflet (Figure 8D). In control experiments with HeLa cells transfected only with membrane proteins but without annexin A4 overexpression, treatment with ionomycin partially reduced mobility of the membrane proteins or had no effect (GPI-EYFP). This partial effect could also be observed in N1E-115 cells (Figure 8E). Most likely, different endogenous annexins were responsible for this effect. Based on these experiments, it can be concluded that annexin A4 strongly influences general plasma membrane protein mobility in a Ca^{2+}-dependent manner.

DISCUSSION

Annexin A4 Localization and Translocation

We constructed fusions of annexin A4 and fluorescent proteins that allowed monitoring dynamic localization of annexin A4 in living cells. The localization and translocation of annexin A4, observed in three different cell lines, is in agreement with previously published results (Barwise and Walker, 1996; Raynal *et al.*, 1996). In addition, we observed that translocation of nuclear annexin A4 always follows the translocation of the cytosolic protein, mostly with a delay of 30 s to 2 min. The reason for the delay may be either the difference in Ca^{2+} concentration between the cytosol and the nucleus or the difference in phospholipid composition of the plasma and the nuclear membrane. Annexin A4 has in fact been shown to exhibit selectivity for particular phospholipids in vitro, for instance, phosphatidylserine (Blackwood and Ernst, 1990; Edwards and Crumpton, 1991; Junker and Creutz, 1994; Sohma *et al.*, 2001).

Cores of several annexins lacking the N-terminal regulatory domain have been observed to have different localization preferences than wild-type proteins (Rescher *et al.*, 2000; Eberhard *et al.*, 2001). We could not observe any difference between the wild-type annexin A4 localization and localization of its core N-terminally fused to a fluorescent protein. Therefore, it appears from our experiments that the interaction of annexin A4 with cellular membranes in living cells does not require the presence of the N-terminal domain and that the core of the protein is sufficient for complete protein translocation upon elevation of $[Ca^{2+}]_i$. Consequently, we do not expect that membrane binding is regulated by phosphorylation of the N-terminal domain, as is described for some annexins (Gerke and Moss, 2002). In vitro data with phosphorylated annexin A4 support this conclusion (Kaetzel *et al.*, 2001).

Annexin A4 Self-Association

Annexin A4 self-association was, until now, observed only in vitro (Zaks and Creutz, 1991). To investigate this process in living cells, we first used the approach described by van der Wal *et al.* (2001). These authors used ratiometric imaging of CFP- and YFP-tagged PH domains to monitor $PI(4,5)P_2$ levels and its breakdown by phospholipase C. They observed about a 30% higher YFP/CFP ratio when the PH domains were membrane bound. We used ECFP- and EYFP-labeled annexin A4 and measured up to a 300% increase in emission ratio upon Ca^{2+}-induced protein translocation to the cellular membranes. This strong increase probably reflects the tight packing of molecules because of protein–protein interactions and the completeness of translocation. Still, we could not entirely exclude the possibility that the FRET raise is a result of increase of the effective protein concentration when docking to the 2D membrane surface and random molecular interaction.

To avoid the problem of unequal expression levels of singly labeled annexin A4, we designed the double-tagged FRET sensor, CYNEX4. Ratiometric EYFP/ECFP imaging of CYNEX4 gave up to 150% increase upon protein translocation. The ratio change is smaller than that obtained with singly labeled proteins, as there is already a significant amount of intramolecular FRET in the absence of Ca^{2+}. This was confirmed by acceptor bleaching experiments. CYNEX4 used in parallel with the Fura red Ca^{2+} sensor demonstrated that $[Ca^{2+}]_i$ rises preceded protein translocation. Translocation was delayed possibly because a certain Ca^{2+} threshold had to be reached.

CYNEX4 was applied in an experiment designed to reveal the origin of the FRET signal upon translocation. We correlated the expression level of CYNEX4 to the FRET increase upon membrane binding in HeLa cells. In case of random interaction, we were expecting linear dependency of energy transfer efficiency and protein concentration. On the other hand, if annexin A4 was self-associating, FRET efficiency would be independent of CYNEX4 concentration (Zaks and Creutz, 1991). The distribution we obtained was neither linearly dependent nor independent of protein concentration. The reason for this is most likely the expression of endogenous annexin A4 in HeLa cells. The latter could interact with CYNEX4 and compete in complex and array formation. At a lower CYNEX4 concentration endogenous protein diluted the CYNEX4 fraction in the arrays, resulting in less FRET. The opposite happened in cells expressing high levels of CYNEX4. In N1E-115 cells endogenous annexin A4 was not detected, and FRET efficiency was not dependent on CYNEX4 concentration as in HeLa cells. Therefore, we conclude that annexin A4 indeed self-associates in living cells. This was further confirmed by FRAP experiments: annexin A4 showed minimal mobility after translocation and hence a very different behavior compared with the PH domain of PLCδ1.

Annexin A4 Effect on Membrane Proteins

One of the consequences of such immobile array formation on the inner leaflet of the plasma membrane may be inhibition of mobility of other membrane proteins. We tested this hypothesis using four different membrane proteins. Mobility of all proteins, except GPI-EYFP, was indeed severely affected in HeLa cells overexpressing annexin A4, after its translocation to the plasma membrane. However, we could also observe ionomycin-induced reduction of mobility in cells not overexpressing annexin A4. It is likely that endogenous annexin A4 and other annexins are responsible for this effect. We demonstrated that annexin A4 is present in HeLa cells (Figure 6D), and at least two other members of the annexin family were previously identified in the same cell type (Sullivan *et al.*, 2000; Grewal *et al.*, 2005). The variability observed in these experiments would reflect the heterogeneity in the Ca^{2+} response, the variability of annexin expression and the efficiency of their translocation. Still, we cannot exclude the existence of another, yet unknown Ca^{2+}-dependent mechanism that regulates membrane protein mobility, because a partially inhibitory effect was observed also in N1E-115 cells that do not express endogenous annexin A4. Nonetheless, the fact that complete annexin A4 translocation results in strong membrane pro-

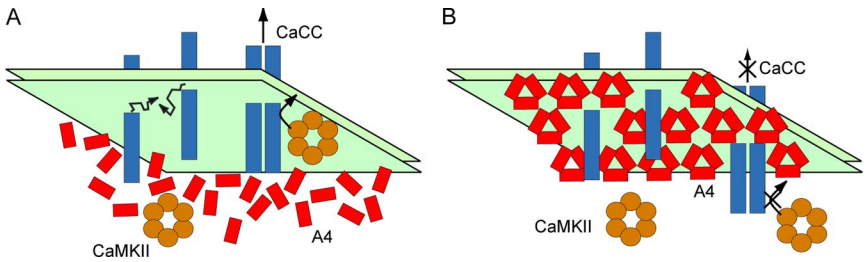

Figure 9. A model for annexin A4–mediated regulation of CaCC. (A) Subunits of a single channel, or different channels, interact to form a functional CaCC (blue). As $[Ca^{2+}]_i$ elevates, CaCC is activated by CaMKII (orange) phosphorylation. (B) Further increase in $[Ca^{2+}]_i$ causes annexin A4 translocation and self-association on the membrane surface. The arrays may prevent the diffusion of Cl^- channel subunits, assembly of a functional channel, and sterically hinder the phosphorylation by CaMKII, leading to inactivation of CaCC.

tein immobilization suggests that this may be one of annexin A4 functions. Annexin A4 is therefore, if not the sole regulator, at least part of a more complex Ca^{2+}-dependent protein mobility regulation mechanism. This function would by no means be exclusive for annexin A4. Any other member of the annexin family with similar array-forming properties could have the same impact on membrane protein mobility. Depending on tissue distribution, expression levels, and subcellular localization, these annexins could interfere with processes depending on membrane protein–protein interaction (e.g., receptor tyrosine kinase dimerization and growth factor signaling). The regulation of membrane protein mobility through annexin A4 arrays may be physiologically relevant in the context of epithelial Ca^{2+}/CaMKII-dependent Cl^- secretion. Annexin A4 is known to inhibit CaCC (Chan *et al.*, 1994; Kaetzel *et al.*, 1994; Xie *et al.*, 1996). Previously Chan *et al.* (1994) proposed that annexin A4 arrays could sterically hinder CaMKII and prevent channel phosphorylation, leading to inhibition of Cl^- conductance. However, the identity of the channels responsible for the Ca^{2+}-activated Cl^- conductance still remains unclear, with several potential candidates, such as Ca^{2+}-activated Cl^- channels and bestrophins. It is therefore possible that, by interacting with each other, several proteins contribute to the observed Ca^{2+}-activated Cl^- current (Fuller *et al.*, 2005). Thus, inhibition of mobility and interaction of those channels may be another level of annexin A4–mediated regulation of epithelial Cl^- secretion (Figure 9).

One obvious question remains: are the observed phenomena physiologically relevant although they could only be followed after artificial stimulation and not with more physiological agonists? A positive conclusion may be found when subcellular annexin A4 localization, local differences in the Ca^{2+} concentration, and a distinct lipid composition of annexin A4 targeted membranes is considered. For example, annexin A4 has been shown to localize below apical membranes of polarized epithelial cells (CaCC localizes to these membranes). It is therefore conceivable that physiological stimuli leading to Ca^{2+} elevation in those cells (e.g., purinergic receptor activation) may locally raise Ca^{2+} to a level sufficient to permit annexin A4–membrane interaction and annexin A4 to function as is proposed in this work. In addition, high Ca^{2+} levels that occur in emergency situations, for instance, after mechanical stress, may trigger annexin A4 self-association as part of a cellular rescue program to preserve cell surface integrity.

Conclusion and Outlook

Fluorescent protein labeling and fluorescence imaging techniques allowed us to study annexin A4 in living cells. Protein translocation, self-association, and mobility were analyzed. The results indicated that annexin A4 may function as a membrane protein mobility regulator, which may also provide a mechanism of CaCC regulation. The sensor we developed, CYNEX4, may be utilized in the future to study annexin A4 dynamics in a more physiological setup, like polarized epithelia or tissue, or to search for activators or inhibitors of annexin A4 self-association. Certainly, similar sensors could be developed and used to study the function of other members of the annexin family.

ACKNOWLEDGMENTS

We thank T. Zimmermann and S. Terjung of EMBL's Advanced Light Microscopy Facility; H. Stichnoth and N. Heath for cultured cells; K. Jalink, P. Bastiaens, and R. Pepperkok for DNA constructs; and J. Ellenberg and J. Brumbaugh for critical reading of the manuscript. Funding was partially provided by the European Union (LSHG-CT-2003-503259).

REFERENCES

Barwise, J. L., and Walker, J. H. (1996). Annexins II, IV, V and VI relocate in response to rises in intracellular calcium in human foreskin fibroblasts. J. Cell Sci. *109*(Pt 1), 247–255.

Blackwood, R. A., and Ernst, J. D. (1990). Characterization of Ca^{2+}-dependent phospholipid binding, vesicle aggregation and membrane fusion by annexins. Biochem. J. *266*, 195–200.

Carew, M. A., Yang, X., Schultz, C., and Shears, S. B. (2000). myo-inositol 3,4,5,6-tetrakisphosphate inhibits an apical calcium-activated chloride conductance in polarized monolayers of a cystic fibrosis cell line. J. Biol. Chem. *275*, 26906–26913.

Chan, H. C., Kaetzel, M. A., Gotter, A. L., Dedman, J. R., and Nelson, D. J. (1994). Annexin IV inhibits calmodulin-dependent protein kinase II-activated chloride conductance. A novel mechanism for ion channel regulation. J. Biol. Chem. *269*, 32464–32468.

Davidson, F. F., Dennis, E. A., Powell, M., and Glenney, J. R., Jr. (1987). Inhibition of phospholipase A2 by "lipocortins" and calpactins. An effect of binding to substrate phospholipids. J. Biol. Chem. *262*, 1698–1705.

Dreier, R., Schmid, K. W., Gerke, V., and Riehemann, K. (1998). Differential expression of annexins I, II and IV in human tissues: an immunohistochemical study. Histochem. Cell Biol. *110*, 137–148.

Eberhard, D. A., Karns, L. R., VandenBerg, S. R., and Creutz, C. E. (2001). Control of the nuclear-cytoplasmic partitioning of annexin II by a nuclear export signal and by p11 binding. J. Cell Sci. *114*, 3155–3166.

Edwards, H. C., and Crumpton, M. J. (1991). Ca^{2+}-dependent phospholipid and arachidonic acid binding by the placental annexins VI and IV. Eur. J. Biochem. *198*, 121–129.

Fuller, C. M., Kovacs, G., Anderson, S. J., and Benos, D. J. (2005). The CLCAs: proteins with ion channel, cell adhesion and tumor suppressor functions. In: Defects of Secretion in Cystic Fibrosis, ed. C. Schultz, New York: Springer Science + Business Media, 83–102.

Gerke, V., Creutz, C. E., and Moss, S. E. (2005). Annexins: linking Ca^{2+} signalling to membrane dynamics. Nat. Rev. Mol. Cell Biol. *6*, 449–461.

Gerke, V., and Moss, S. E. (2002). Annexins: from structure to function. Physiol. Rev. *82*, 331–371.

Gerke, V., and Weber, K. (1984). Identity of p36K phosphorylated upon Rous sarcoma virus transformation with a protein purified from brush borders; calcium-dependent binding to non-erythroid spectrin and F-actin. EMBO J. *3*, 227–233.

Gilmanshin, R., Creutz, C. E., and Tamm, L. K. (1994). Annexin IV reduces the rate of lateral lipid diffusion and changes the fluid phase structure of the lipid bilayer when it binds to negatively charged membranes in the presence of calcium. Biochemistry *33*, 8225–8232.

Grewal, T. *et al.* (2005). Annexin A6 stimulates the membrane recruitment of p120GAP to modulate Ras and Raf-1 activity. Oncogene *24*, 5809–5820.

Ho, M. W., Kaetzel, M. A., Armstrong, D. L., and Shears, S. B. (2001). Regulation of a human chloride channel. A paradigm for integrating input from calcium, type II calmodulin-dependent protein kinase, and inositol 3,4,5,6-tetrakisphosphate. J. Biol. Chem. *276*, 18673–18680.

Junker, M., and Creutz, C. E. (1994). Ca^{2+}-dependent binding of endonexin (annexin IV) to membranes: analysis of the effects of membrane lipid composition and development of a predictive model for the binding interaction. Biochemistry *33*, 8930–8940.

Kaetzel, M. A., Chan, H. C., Dubinsky, W. P., Dedman, J. R., and Nelson, D. J. (1994). A role for annexin IV in epithelial cell function. Inhibition of calcium-activated chloride conductance. J. Biol. Chem. *269*, 5297–5302.

Kaetzel, M. A., Hazarika, P., and Dedman, J. R. (1989). Differential tissue expression of three 35-kDa annexin calcium-dependent phospholipid-binding proteins. J. Biol. Chem. *264*, 14463–14470.

Kaetzel, M. A., Mo, Y. D., Mealy, T. R., Campos, B., Bergsma-Schutter, W., Brisson, A., Dedman, J. R., and Seaton, B. A. (2001). Phosphorylation mutants elucidate the mechanism of annexin IV-mediated membrane aggregation. Biochemistry *40*, 4192–4199.

Kourie, J. I., and Wood, H. B. (2000). Biophysical and molecular properties of annexin-formed channels. Prog. Biophys. Mol. Biol. *73*, 91–134.

Lippincott-Schwartz, J., Snapp, E., and Kenworthy, A. (2001). Studying protein dynamics in living cells. Nat. Rev. Mol. Cell Biol. *2*, 444–456.

Llopis, J. *et al.* (2000). Ligand-dependent interactions of coactivators steroid receptor coactivator-1 and peroxisome proliferator-activated receptor binding protein with nuclear hormone receptors can be imaged in live cells and are required for transcription. Proc. Natl. Acad. Sci. USA. *97*, 4363–4368.

Mayran, N., Traverso, V., Maroux, S., and Massey-Harroche, D. (1996). Cellular and subcellular localizations of annexins I, IV, and VI in lung epithelia. Am. J. Physiol. *270*, L863–L871.

Newman, R. H., Leonard, K., and Crumpton, M. J. (1991). 2D crystal forms of annexin IV on lipid monolayers. FEBS Lett. *279*, 21–24.

Raynal, P., Kuijpers, G., Rojas, E., and Pollard, H. B. (1996). A rise in nuclear calcium translocates annexins IV and V to the nuclear envelope. FEBS Lett. *392*, 263–268.

Rescher, U., and Gerke, V. (2004). Annexins—unique membrane binding proteins with diverse functions. J. Cell Sci. *117*, 2631–2639.

Rescher, U., Zobiack, N., and Gerke, V. (2000). Intact Ca^{2+}-binding sites are required for targeting of annexin 1 to endosomal membranes in living HeLa cells. J. Cell Sci. *113*(Pt 22), 3931–3938.

Sohma, H., Creutz, C. E., Gasa, S., Ohkawa, H., Akino, T., and Kuroki, Y. (2001). Differential lipid specificities of the repeated domains of annexin IV. Biochim. Biophys. Acta *1546*, 205–215.

Sullivan, D. M., Wehr, N. B., Fergusson, M. M., Levine, R. L., and Finkel, T. (2000). Identification of oxidant-sensitive proteins: TNF-alpha induces protein glutathiolation. Biochemistry *39*, 11121–11128.

Vajanaphanich, M., Schultz, C., Rudolf, M. T., Wasserman, M., Enyedi, P., Craxton, A., Shears, S. B., Tsien, R. Y., Barrett, K. E., and Traynor-Kaplan, A. (1994). Long-term uncoupling of chloride secretion from intracellular calcium levels by Ins(3,4,5,6)P4. Nature *371*, 711–714.

van der Wal, J., Habets, R., Varnai, P., Balla, T., and Jalink, K. (2001). Monitoring agonist-induced phospholipase C activation in live cells by fluorescence resonance energy transfer. J. Biol. Chem. *276*, 15337–15344.

Violin, J. D., Zhang, J., Tsien, R. Y., and Newton, A. C. (2003). A genetically encoded fluorescent reporter reveals oscillatory phosphorylation by PKC. J. Cell Biol. *161*, 899–909.

Weber, K., Johnsson, N., Plessmann, U., Van, P. N., Soling, H. D., Ampe, C., and Vandekerckhove, J. (1987). The amino acid sequence of protein II and its phosphorylation site for PKC; the domain structure Ca^{2+}-modulated lipid binding proteins. EMBO J. *6*, 1599–1604.

Willshaw, A., Grant, K., Yan, J., Rockliffe, N., Ambavarapu, S., Burdyga, G., Varro, A., Fukuoka, S., and Gawler, D. (2004). Identification of a novel protein complex containing annexin A4, rabphilin and synaptotagmin. FEBS Lett. *559*, 13–21.

Wouters, F. S., Verveer, P. J., and Bastiaens, P. I. (2001). Imaging biochemistry inside cells. Trends Cell Biol. *11*, 203–211.

Xie, W., Kaetzel, M. A., Bruzik, K. S., Dedman, J. R., Shears, S. B., and Nelson, D. J. (1996). Inositol 3,4,5,6-tetrakisphosphate inhibits the calmodulin-dependent protein kinase II-activated chloride conductance in T84 colonic epithelial cells. J. Biol. Chem. *271*, 14092–14097.

Xie, W., Solomons, K. R., Freeman, S., Kaetzel, M. A., Bruzik, K. S., Nelson, D. J., and Shears, S. B. (1998). Regulation of Ca^{2+}-dependent Cl^- conductance in a human colonic epithelial cell line (T84): cross-talk between Ins(3,4,5,6)P_4 and protein phosphatases. J. Physiol. *510*(Pt 3), 661–673.

Zaks, W. J., and Creutz, C. E. (1991). Ca^{2+}-dependent annexin self-association on membrane surfaces. Biochemistry *30*, 9607–9615.

Zanotti, G., Malpeli, G., Gliubich, F., Folli, C., Stoppini, M., Olivi, L., Savoia, A., and Berni, R. (1998). Structure of the trigonal crystal form of bovine annexin IV. Biochem. J. *329*(Pt 1), 101–106.